Comprehensive synthesis of monohydroxy-cucurbit[*n*]urils (*n* = 5, 6, 7, 8): high purity and high conversions.

Mehmet M. Ayhan,[†,‡] Hakim Karoui,[†] Micaël Hardy,[†] Antal Rockenbauer,[Ω] Laurence Charles,[†] Roselyne Rosas,[Δ] Konstantin Udachin,[Π] Paul Tordo,[†] David Bardelang[†*] and Olivier Ouari.[†*]

[†]Aix-Marseille Université, CNRS, Institut de Chimie Radicalaire, UMR 7273, 13397 Marseille, France, [‡], Department of Chemistry, Gebze Technical University, P.K.:141, 41400 Gebze, Kocaeli, Turkey, [Ω] Institute of Materials and Environmental Chemistry, Hungarian Academy of Sciences; Department of Physics, Budapest University of Technology and Economics, Budafoki ut 8, 1111 Budapest, Hungary, [Δ]Aix-Marseille Université, CNRS, Spectropole, FR 1739, 13013 Marseille, France, [Π]National Research Council Canada, 100 Sussex Drive, Ottawa, ON, K1A 0R6, Canada.

ABSTRACT: We describe a photochemical method to introduce a single alcohol function directly on cucurbit[*n*]urils (*n* = 5, 6, 7, 8) with conversions of the order 95-100% using hydrogen peroxide and UV light. The reaction was easily scaled up to 1 gram for CB[6] and CB[7]. Spin trapping of cucurbituril radicals combined with MS experiments allowed us to get insights about the reaction mechanism and characterize CB[5], CB[6], CB[7] and CB[8] monofunctional compounds. Experiments involving ^{18}O isotopically labeled water indicated that the mechanism was complex and showed signs of both radical and ionic intermediates. DFT calculations allowed estimating the Bond Dissociation Energies (BDEs) of each hydrogen atom type in the CB series, providing an explanation of the higher reactivity of the 'equatorial' C-H position of CB[*n*] compounds. These results also showed that, for CB[8], direct functionalization on the cucurbituril skeleton is more difficult because one of the methylene hydrogen atoms (Hb) has its BDE lowering within the series and coming close to that of Hc thus opening the way to other types of free radicals generated on the CB[8] skeleton leading to several side-products. Yet CB[5]-$(OH)_1$ and CB[8]-$(OH)_1$, the first CB[8] derivative, were obtained in excellent yields thanks to the soft method presented here.

INTRODUCTION

Cucurbit[*n*]urils (CB[*n*])[1] belong to a growing family of synthetic macrocycles displaying many unprecedented properties. Among them, the exceptional recognition abilities of CB[7],[2] or the formation of charge-transfer ternary complexes of CB[8][3] enabling the non-covalent "clicking" of dendrimers,[4] peptides,[5] polymers[6] or proteins[7] have opened up new avenues in supramolecular and surface chemistry. While great progresses have been obtained with cucurbiturils, two main limitations still prevent many potential applications.[1] First, the very low solubility of CB[6] and CB[8] in water[8] (< 0.1 mM) and second the challenging task to introduce functional groups on the CB skeletons.[9] Whereas the addition of suitable guests has partially addressed the former point,[10] the preparation of functionalized cucurbiturils remains difficult for CB[7] and has still to be reported for CB[8].[11] Due to the rather small size of the CB[6] cavity, monofunctional higher size cucurbiturils are highly desirable in order to open up new supramolecular perspectives where larger containers are required. In 2011 and 2012, two papers appeared using two different strategies. In the first one, Isaacs used a glycoluril hexamer precursor before reaction with a suitably functionalized glycoluril affording a monofunctional CB[7] in a 5 step sequence.[12] In the second one, Scherman reported the preparation of mono-hydroxylated CB[6][13] using a modified method published earlier by Kim[14] using persulfate salts. Since then, the Kim method has been optimized to obtain monohydroxy CB[7] in one step.[15] However, the reaction conversions are not quantitative, requiring non trivial and time-consuming purification steps, and a monofunctional CB[8] derivative such as CB[8]-(OH) is still missing. Whatever the tedious work, two astonishing applications emerging from functionalized CBs were reported recently. In the first one, Kim used monofunctional CB[7]-(OH) to graft CB[7] on a solid support and designed a complementary surface carrying ferrocenium groups enabling the construction of a supramolecular Velcro working under water.[15] In the second work, Isaacs introduced a single functional group outside the skeleton of CB[7] to target cancer cells while preserving the cavity available for drug transportation.[12d] Herein, we report a method allowing the easy preparation of monohydroxy-CB[*n*] (CB[*n*]-OH, *n* = 5 to 8) in high yields based on the photoirradiation of hydrogen peroxide in the presence of cucurbiturils in water. We also provide some evidence that the reaction proceeds by hydrogen abstraction of the pseudo-acidic equatorial hydrogen atoms of the CB[*n*] and explain why it has been difficult until now to prepare a monofunctional CB[8] derivative.

RESULTS AND DISCUSSION

Synthesis. Based on the work of Kim et al., we have been interested in testing the UV photolysis of hydrogen peroxide

(λ = 254 nm, Rayonet reactor) as a source of hydroxyl radicals (Scheme 1). Our motivation was based on the use of hydrogen peroxide as the sole reagent, the high efficiency of the reaction, its easy control, and the formation of water only as a side product. Attempts using Fenton reaction (H_2O_2, $FeSO_4$) in the presence of CB[7] were unsuccessful due to the precipitation of the cucurbituril by Fe(II).

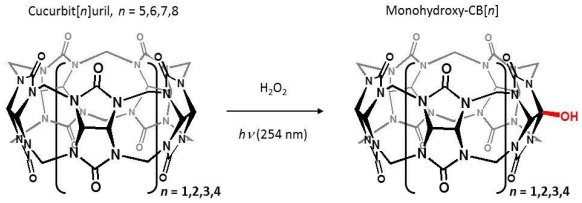

Scheme 1. Synthesis of monohydroxy-cucurbit[*n*]urils.

A series of experiments was performed in water to optimize reaction conditions and one key parameter was the concentration of hydrogen peroxide. Below 1 mM, the reaction hardly produced CB[*n*]-(OH) but on the other hand, at concentrations above 4 mM, a white precipitate formed consisting of degradation products of CB[*n*] containing macrocycles lacking carbon atoms, with or without –OH groups (see MS section below and Figures S1 to S3) and leading to dramatic decreases of the reaction yield. It was then noticed that aqueous HCl improved the homogeneity of the mixture and allowed to extend the reaction to CB[6] and CB[8] which were otherwise hardly soluble in water. Thus, aqueous acidic solutions (HCl, 5 M) were used and the reaction evolution was monitored by ^{1}H NMR after freeze-drying of aliquots. This procedure allowed optimizing the reaction time for almost quantitative conversions (Figure S4, Table 1) thus avoiding difficult purification steps. Longer UV irradiation times generally led to over-hydroxylated products (Figure S1). Typically around 100 mg of each cucurbituril was used affording each monohydroxy analogue in excellent yields (Scheme 1). At the end of the reaction, the solvent was evaporated under reduced pressure using a rotavapor. Furthermore, adding HCl (5M) allowed to scale up the reaction to 1 g of CB[6] for which CB[6]-(OH) was obtained in 2 hours with a purity > 95% as determined by ^{1}H NMR (Figure 1). The reaction works equally well for CB[7] affording 1g of CB[7]-(OH) in 6 hours. This reaction can be repeated to produce several grams of the relevant monohydroxyl-cucurbituril in one day. The data summarized in Table 1 show that almost quantitative conversions were reached for each cucurbituril enabling to use directly the crude product with a purity > 90-95% by ^{1}H NMR for further reactions. For CB[6], using a higher concentration of H_2O_2 in HCl 5M clearly showed that CB[6]-$(OH)_2$ and CB[6]-$(OH)_n$ (n>2) can be obtained also in high yields (Figure S8).

The ^{1}H NMR spectra in D_2O for the series of CB[*n*]-(OH) are reported in Figure 1 and show all integrals to be in line with expectations and correlates well with that already reported for CB[6]-(OH).[13] Compared to the typical three peak, doublet, singlet, doublet, observed in ^{1}H NMR spectra of CB[*n*], a new and characteristic peak is observed in the 5.3 ppm area, assigned to the H atom in equatorial position next to the hydroxyl group grafted on the relevant glycoluril unit (H_a).

Table 1. Reaction conditions and conversions for the preparation of CB[*n*]-$(OH)_1$ (n=5 to 8, λ = 254 nm, 16 light bulbs in Rayonet reactor).

CB[*n*]-$(OH)_1$	CB[*n*] conc.	[H_2O_2]	Conversion*	reaction time
CB[5]-(OH)	2 mM	1 mM	95%	2H
CB[6]-(OH)	2 mM	1 mM	95-100%	2H
CB[7]-(OH)	2 mM	1 mM	95-100%	5H
CB[8]-(OH)	1 mM	0.5 mM	90%**	4H

*: based on ^{1}H NMR. **: purified by recrystallization, Figure S5.

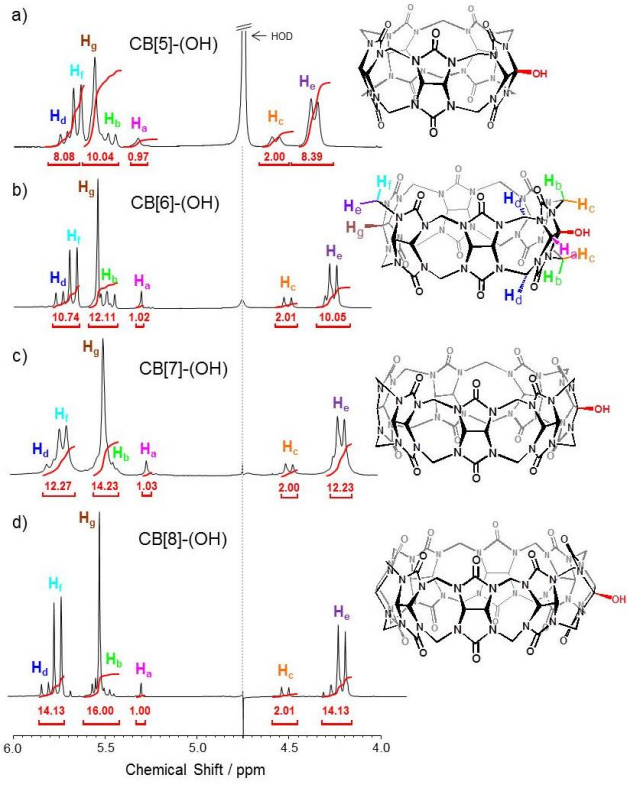

Figure 1. 400MHz ^{1}H NMR spectra in D_2O of CB[5]-(OH), CB[6]-(OH), CB[7]-(OH) and CB[8]-(OH) respectively in a), b), c), and d). Cystamine was used in a), b) and d) for full solubilization.

Furthermore, additional signals are observed due to the symmetry cancelation of the CB skeleton, and the integral values in the CB series are consistent with the expected structures (Figure 1). The structures of CB[*n*]-(OH) were further confirmed by ^{13}C NMR, High Resolution MS analyses and X-ray crystallography (Figure 2 and supporting information Figures S9 to S16). The X-ray diffraction data show a single hydroxyl group disordered over 6 positions for CB[5], 4 positions for CB[6] and 8 positions for CB[8]. This disorder is inherent to the CB structures owing to their symmetry. Calculations of electron densities around the CB skeletons agreed with the structures shown in Figure 2.

Table 2. Bond Dissociation Energies (BDEs) for the C-H bonds corresponding to the abstraction of hydrogen atoms H_a, H_b and H_c from CB[5] to CB[8] leading to cucurbituril radicals.

BDE (kcal.mol^{-1})	H_a abstraction (secondary radical)	H_b abstraction (secondary radical)	H_c abstraction (tertiary radical)	$\Delta_{Hb\text{-}Hc}$ (kcal.mol^{-1})
Structure of the radicals			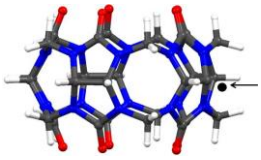	
CB[5] (kcal.mol^{-1})	**101.01**	**95.77**	**88.36**	**7.41**
α angle (°)[a]	65.6	38.0	25.7	
Offset from flatness (Å)	0.25	0.31	0.40	
Σ angles around radical center (°)	349.2	342.9	337.3	
CB[6] (kcal.mol^{-1})	**101.72**	**93.22**	**88.68**	**4.54**
α angle (°)[a]	64.9	29.8	25.7	
Offset from flatness (Å)	0.25	0.29	0.40	
Σ angles around radical center (°)	348.7	344.7	337.0	
CB[7] (kcal.mol^{-1})	**102.81**	**92.00**	**89.05**	**2.95**
α angle (°)[a]	66.0	25.5	25.4	
Offset from flatness (Å)	0.26	0.28	0.40	
Σ angles around radical center (°)	348.4	346.0	337.0	
CB[8] (kcal.mol^{-1})	**103.73**	**91.40**	**89.25**	**2.15**
α angle (°)[a]	67.1	23.0	25.1	
Offset from flatness (Å)	0.26	0.27	0.40	
Σ angles around radical center (°)	348.4	346.9	337.1	

[a] Angle between the SOMO orbital and the 1st and 2nd π N-C-O systems (see Scheme 2).

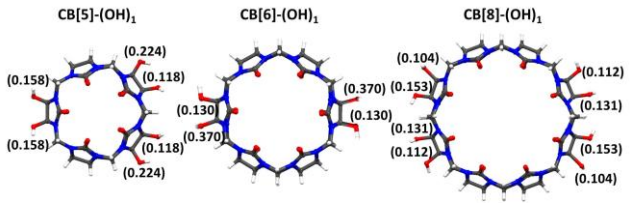

Figure 2. Crystal structures of CB[5]-(OH), CB[6]-(OH) and CB[8]-(OH) with the OH group disordered over 6 positions for CB[5]-(OH), 4 positions for CB[6]-(OH) and 8 positions for CB[8]-(OH) (the % occupancy for each corresponding position is given in parenthesis, guests and solvent removed for clarity).

Several crystal batches of CB[5]-(OH), CB[6]-(OH) and CB[8]-(OH) were prepared but ended up with the same disordered structures. All attempts to crystallize CB[7]-(OH) were unsuccessful. Because the hydroxyl radical is a highly reactive species, we sought for stereo-electronic arguments to rationalize the highly selective hydroxylation at position *c* (Figures 1 and 2 and Table 2) as observed by NMR and X-ray crystallography.[13-15]

DFT calculations: C-H Bond Dissociation Energies. DFT calculations of bond dissociation energies (BDE) of the C-H bonds were performed using the software Gaussian 09 Rev. D01 (Table 2). The geometries of the species were optimized at the B3LYP/6-31G(d) level and vibrational frequencies were calculated at the same level of theory to ensure that the optimized geometries are true minima. The corresponding thermal corrections were included to obtain the enthalpy values under the standard conditions (p = 1 atm and T= 298.15 K). The BDE was calculated by subtracting the enthalpies of the CB centered radical and hydrogen atom radical from that of the relevant cucurbituril. For example, the calculation of the BDE corresponding to the cleavage of hydrogen H_c from CB[7] is equal to $[\Delta H(CB[7]c\bullet) + \Delta H(H\bullet)] - \Delta H(CB[7])$. All three CB[*n*] minus H_a, CB[*n*] minus H_b, and CB[*n*] minus H_c reactions were considered. However, CB[*n*] minus H_a and CB[*n*] minus H_b generate a unique CB[*n*]• species because of the low inversion barrier at the radical center. Nevertheless, we will consider CB[*n*]•-(H_a), CB[*n*]•-(H_b) and CB[*n*]•-(H_c) for the BDE discussion because each reaction is different. H_a, H_b and H_c are carried by carbon atoms which are connected to two nitrogen atoms, but there are two types of radicals after hydrogen abstraction: the products CB[*n*]•-(H_a) and CB[*n*]•-(H_b) are secondary radicals and CB[*n*]•-(H_c) is a more stabilized tertiary radical. Considering only BDE values within the series, the CB[*n*]−H_a bond has the highest energy, of the same order of magnitude than that of the C−H bond in isobutane (*ter*-butyl radical = 96.5 kcal.mol^{-1})[16] and does not change from CB[5] to CB[8] (Table 2). For position H_c, the C−H bond has the lowest energy in the series, because of the tertiary feature of the radical and of the allylic character due to the partial delocalization of the unpaired electron on the two adjacent nitrogen atoms involved in two urea functions. The BDE of CB[*n*]−H_c stays

nearly constant within the series CB[5] to CB[8] (from 88.4 to 89.3 kcal.mol^{-1}). For position H_b however, the BDE in CB[5] is of the same order of magnitude as that of H_a but the BDE value decreases in the series from 95.8 to 91.4 kcal.mol^{-1} going from CB[5] to CB[8]. This trend can be due to a gradually stabilizing effect of the radical and loosening of the C-H bond due to an improved delocalization ability of the radical when going from CB[5] to CB[8]. When looking at the angle α between the Single-Occupied Molecular Orbital (SOMO) of the radical and the π systems next to it in the series (Scheme 2), this angle does not change from CB[5] to CB[8] for positions H_a and H_c with values of 65.9±1.2° and 25.5±0.4° respectively.

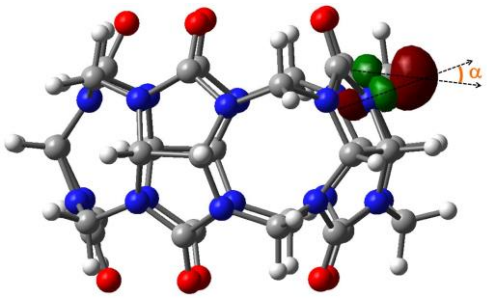

Scheme 2. α angle between the SOMO orbital of the CB[5]•-H_b free radical and the π system of the adjacent nitrogen atoms.

However, for H_b, this angle decreases from 38 to 23° progressively, increasing the allylic character of the radical thus loosening the corresponding C-H bond (BDE of allylic C-H bond: 96.7 kcal.mol^{-1}). Thus, even being the source of a secondary radical, the BDE of CB[*n*]−H_b is decreasing within the series until reaching a BDE value close to the one of CB[*n*]−H_c in CB[8]. This small BDE difference could be at the origin of the more tedious hydroxylation of CB[8][14] with H atom abstraction reactions occurring not exclusively at the *c* position but also at position *b* which is more prone to evolve to decay products (ring opening and missing methylene bridges, *vide infra*). The SOMO of the CB[8]•-(H_c) radical shows a substantial delocalization of its electron in the two nitrogen containing π systems of the neighboring ureidic groups. The sum of angles around the radical center which reflects the offset from flatness stays constant within the series. These data reflect that the pyramidalization character is not cucurbituril dependent and that the CB radical corresponding to H_c abstraction is a little more pyramidal, most probably as a consequence of the cyclic strain imposed by the cucurbituril ring structure on this tertiary radical.

From DFT calculations, the selectivity in the H atom abstraction by hydroxyl radicals appears more clearly, with a more likely H_c hydrogen abstraction position for CB[*n*]. With a BDE of the order of 88-89 kcal.mol^{-1}, the other two bonds have higher energies at 91-96 and 101-104 kcal.mol^{-1} for H_b and H_c respectively. These results bring insights on the favored 'equatorial' position functionalization as also reported by Kim for the per-hydroxylation of cucurbit[*n*]urils (*n* = 5 to 8),[14] and could in part explain the CB[8] ring structure regarding direct functionalization.

EPR-Spin Trapping and High Resolution MS. Beside the work of Kim[14,15] and Scherman[13] on cucurbituril hydroxylation, another team has recently reported the immobilization of CB[7] on solid supports *via* a photochemical reaction with azido groups[17] but little was reported concerning the underlying mechanism. Likewise, Fuenzalida and Fuentealba reported protection of encapsulated dyes against photodegradation by radicals generated by the Fenton reaction.[18]

As part of our work on cucurbiturils[19] and on the development of the EPR - spin trapping technique for the characterization of transient free radicals,[20,21] we performed a series of experiments where spin traps were added to the hydroxylation reaction of CBs in order to get indirect evidence for the formation of CB[7]• or CB[8]• radicals. Nitroxide spin adducts are generated and their paramagnetic character allowed to investigate the radical trapped by EPR spectroscopy (Figure 3a).

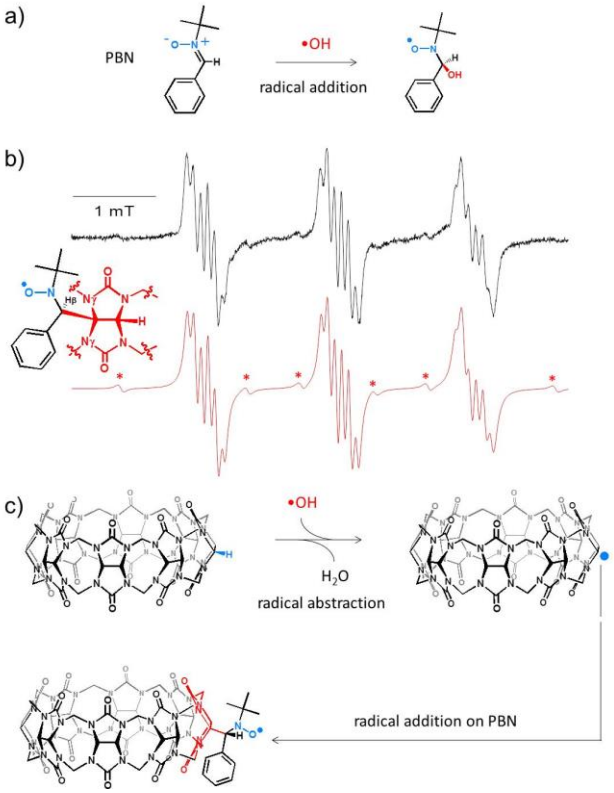

Figure 3. (a) Spin trapping of HO• radical by PBN. (b) Experimental EPR spectrum (black) and simulation (red) after spin trapping of the hydroxyl radical by PBN in the presence of CB[8]. Simulations indicate a 33/64 ratio of PBN-•OH and PBN-•CB[8] nitroxides spin adducts respectively. The star is for an unknown paramagnetic species accounting for ~3% of the signal. (c) Proposed spin trapping scheme of the CB[8]• radical.

A set of nitrone spin traps was investigated and among them, the linear molecules (PBN and PyOBN) gave the most useful EPR spectra (Figure 3) as compared with cyclic analogues (DMPO or DIPPMPO,[22] spin trap structures in supporting information). Using PBN as spin trap, the signals are well resolved in the case of CB[8] (Figure 3), and the assignment of the spectra can be satisfactorily simulated assuming the superposition of the signal of the HO-spin adduct of PBN (PBN-

OH), (a_N = 1.64 mT; $a_{H\beta}$ = 0.28 mT) and a second spin adduct. This second spin adduct has EPR features of a carbon fragment connected to two equivalent nitrogen atoms (a_N = 1.62 mT, $a_{H\beta}$ = 0.095 mT, $a_{N\gamma}$ (2 N_γ) = 0.08 mT, Figure 3b). This represents the first spin labelled cucurbituril and this nitroxide is persistent. The very small β-coupling indicates that the β-hydrogen lies in the nodal plane of the nitroxide group and this geometry together with the steric hindrance of the cucurbituril moiety likely prevent a rapid disproportionation of the nitroxide (Figure 3c). To confirm the presence of the PBN nitrone in solution and not as an inclusion complex in CBs, control ^{1}H NMR titrations were performed and showed that the binding of PBN toward CB[7] is weak ($K_{a\ 293K} \approx 189\ M^{-1}$, yielding only 8% of complexed PBN under the conditions of EPR experiments). Similarly, no significant complexation-induced shifts were observed in ^{1}H NMR spectra with CB[8], in line with a low binding toward CB[8]. To get further details on the structures of CB[*n*]• radical, we used nitroxides to trap the generated radical. TEMPO nitroxides are known to react with carbon centered radicals at rates ~ 10^7-10^8 $M^{-1}.s^{-1}$ to produce stable alkoxyamines.[23] When the stable free radical 4-methoxy-2,2,6,6-tetramethylpiperidinyloxy (4M-TEMPO after referred to as **4M**) was added (4 mM) to a mixture containing CB[7] (2 mM) and H_2O_2 (2 mM), after UV irradiation, MS analyses indicated that **4M** acted as a trapping agent for the CB[7]• radical. Indeed, due to the bimolecular character of the addition reaction and of the small steady state concentration of CB• radical, a small amount of diamagnetic adduct is formed but still detectable by MS. In ESI-MS experiments, a peak corresponding to the sum of the masses of **4M** and CB[7] minus one hydrogen was detected and unambiguously assigned to a covalent CB[7] adduct because the non covalent complex **4M**@CB[7] would have shown a mass with one mass atomic unit more. Therefore, the peak at *m/z* 691.7765 (calc. *m/z* 691.7764) corresponds to the species [CB[7]-H+**4M**+2NH_4]$^{2+}$ (elemental composition: $C_{52}H_{69}N_{31}O_{16}^{2+}$) and clearly supports the trapping of a CB[7]• radical by nitroxide **4M** (supporting information Figure S17). This result agrees well with the observed monohydroxylated product observed by MS for the CB[7]/HO• system alone. Similar results were obtained with TEMPO as trapping agent (supporting information).

Hydroxylation and decay reactions. As shown in Table 3, the best hydrogen peroxide concentration for CB[8] monohydroxylation is 0.5 mM. Above this concentration, additional products are seen by NMR in the form of additional broad signals in the CB region. Table 3 highlights the influence of hydrogen peroxide concentration and reaction time on the reaction distribution products. Other parameters were investigated and it was found that a number of 16 light bulbs gave the highest conversions. Magnetically stirring was also important as was the influence of oxygen (O_2) dissolved in the mixture since either not stirring or bubbling oxygen prior to the reaction resulted in either slower kinetics or detection of side-products respectively (Figure S19).

To get further insights on the side-products formed during the reaction, high-resolution MS analyses were performed for a sample where CB[8] was subjected to UV irradiation in the presence of H_2O_2 at 5.6 mM.

Table 3. Conversion of CB[8] toward the formation of CB[8]-$(OH)_1$ (λ = 254 nm, 16 light bulbs in Rayonet reactor, CB[8] concentration 2 mM except 1 mM for $[H_2O_2]$=0.5 mM).

Time/min	$[H_2O_2]$ / 5.6 mM	$[H_2O_2]$ / 2.8 mM	$[H_2O_2]$ / 2.0 mM	$[H_2O_2]$ / 0.5 mM
10	~30%*	12%	10%	5%
20	~40%*	20%	20%	10%
30	~50%*	~30%*	25%	15%
40	~60%*	~50%*	~35%*	15%
50	~80%*	~70%*	~50%*	20%
60	~100%*	~80%*	~70%*	30%
70		~100%*	~80%*	50%
80			~100%*	65%
90				70%
100				80%
110				90%
120				100%
130				~100%*

*: additional products as detected by ^{1}H NMR.

Because cucurbiturils with missing carbons on the glycoluril moiety were never observed, we postulated the vacancy of one or two methylene bridging carbons as reported for nor-seco cucurbituril analogues by Isaacs.[24] Results are shown in Figure 4 after addition of cystamine to ensure solubilization of all possible compounds similar in structure to CB[8]. Consequently, all peaks are measured as cystamine adducts in the form [CB*+cystamine+2H]$^{2+}$. On the basis of the elementary composition determined by high-resolution MS measurements (supporting information Table S7), the different ions with structures given in Figure 4 were proposed. Beside expected peaks for CB[8] (species number 4, *m/z* 741.2259) and CB[8]-(OH) (*m/z* 749.2235), there is a number of other compounds, hydroxylated, with missing carbons, or both. For example nor-seco analogues with one (species 2, *m/z* 735.2257) or two (species 1, *m/z* 729.2260) missing carbon atoms were detected. For symmetry reasons, species 2 is unique but there are no reasons for species 1 why two missing carbons would be adjacent or affording symmetrical products. Accordingly, mixtures for which the positions of missing carbons are random are expected. Other analogues with one, two or three –OH groups are also detected. There are also peaks which can be assigned to different isomeric species where functional groups are different (Figure 4, species 6, 8, 10 and 12, supporting information).[25] Thus, it appears that the generation of the hydroxyl radicals by UV photolysis of hydrogen peroxide has to be well-balanced in order to avoid the formation of over-oxidized products and to control the kinetics of the competitive reactions. Finally, we observed slight differences among cucurbiturils, especially for CB[8] where, depending on CB[8] batches, the optimal reaction time was adjusted between 2 and 4 hours. Because cucurbiturils radicals are formed rapidly at the beginning of the reaction, direct functionalization was assessed by trapping the CB-based radical by an acrylate monomer. Maleic anhydride (MA) was then added in the reaction medium because of its propensity to avoid homopolymerization.

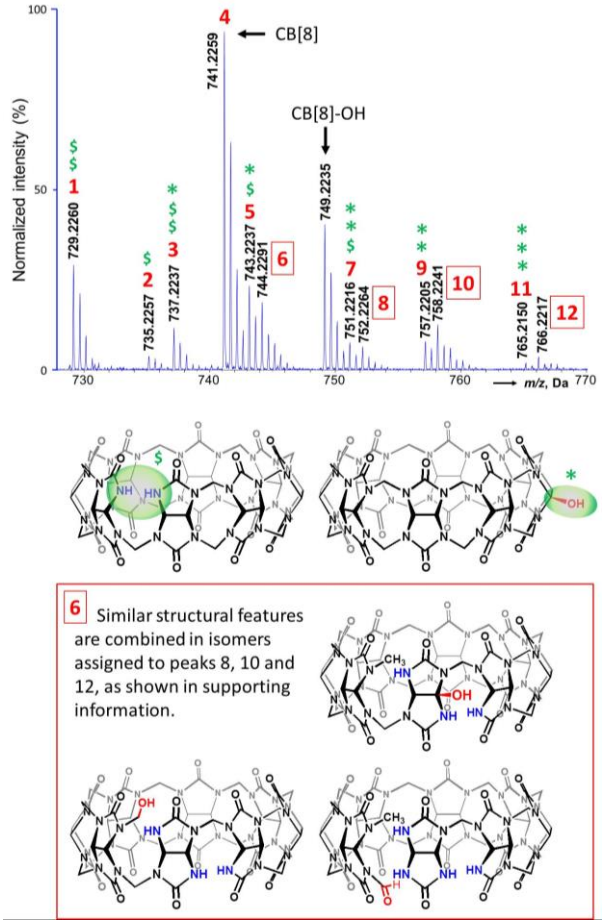

Figure 4. High-Resolution electrospray mass spectrum after reaction of CB[8] with H_2O_2 (5.6 mM in HCl 5M after freeze-drying), of the redissolved mixture using cystamine. Possible chemical modifications are shown as the $ or the * symbols (random position of the modification is expected). Cases were several other isomers can be envisioned are for peaks 6, 8, 10 and 12 for which other possible structures are shown at the bottom (6) and in the supporting information (8, 10 and 12).

Unfortunately, no direct grafting could be observed irrelevant of the quantity of MA added.

Isotopically labeled CB[7]-(^{18}OH). In order to get further details on the full mechanism of the hydroxylation step, ^{18}O isotopically labeled water ($H_2{}^{18}O$, 96% ^{18}O) was employed to assess the radical or ionic character of the hydroxylation step using ESI HRMS experiments (Scheme 3).

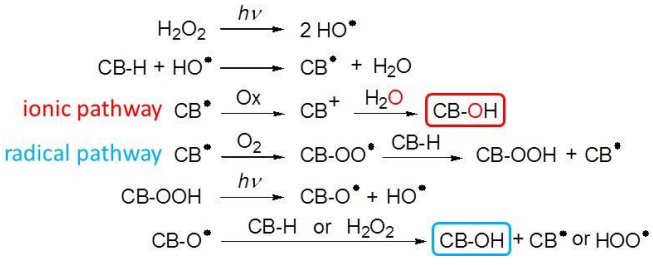

Scheme 3. Possible radical and ionic mechanisms leading to CB[*n*]-(OH).

From HR-MS analyses, a 37/63 ratio was obtained with the unlabelled CB[*n*]-^{16}OH formed as the major product, indicating that both mechanisms seems to contribute, with a major extend on the ionic mechanism (Figure 5).

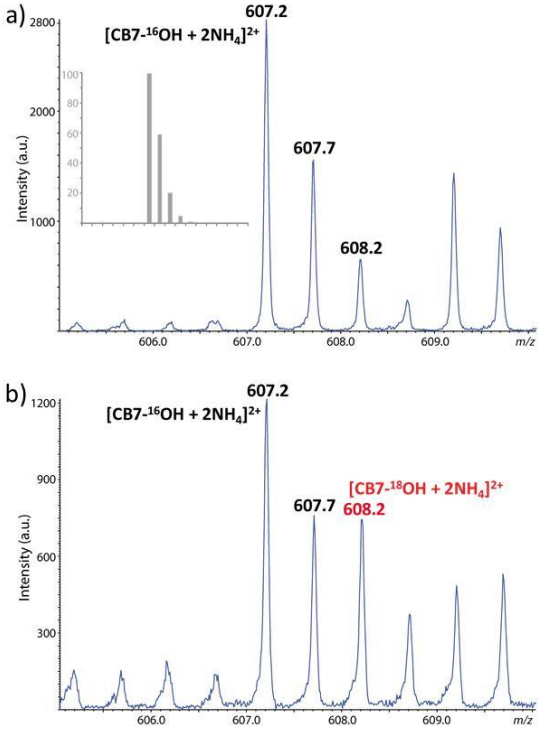

Figure 5. ESI mass spectrum (excerpt on the 605-610 *m/z* range) obtained for a) sample A, experiment using $H_2{}^{16}O$ and b) sample B (experiment using $H_2{}^{18}O$, see SI). Inset: theoretical isotopic pattern of $[CB[7]\text{-}(OH)_1+2NH_4]^{2+}$ ($C_{42}H_{50}N_{30}O_{15}{}^{2+}$).

In order to perform relative quantification of isotopically labeled and unlabeled species, which only differ by 1 m/z unit and hence yield interfering isotopic patterns, the following correcting procedure was implemented. In Figure 5b, the third isotopic peak of CB[7]-(^{16}OH) and the first isotopic peak of CB[7]-(^{18}OH) both contribute to the signal at *m/z* 608.2. Nonetheless, individual contribution of each species can be estimated since the intensity of the third isotopic peak of CB[7]-(^{16}OH) can be predicted based on the intensity measured for the first isotopic peak of CB[7]-(^{16}OH) at *m/z* 607.2. Theoretical intensity ratio of peaks at *m/z* 608.2 and *m/z* 607.2 in the isotopic pattern of $C_{42}H_{50}N_{30}O_{15}{}^{2+}$ is 20.11%. The experimental I(*m/z* 608.2)/I(*m/z* 607.2) ratio, found to be equal to 26.32% ± 0.95 (95% confidence, supporting information), was then used to estimate the contribution of CB[7]-(^{16}OH) to the peak at *m/z* 608.2 based on intensity measured for CB[7]-(^{16}OH) at *m/z* 607.2 in a set of ten replicate analyses. Finally, so-obtained data were subtracted from measured I(*m/z* 608.2) values to reach the actual contribution of CB[7]-(^{18}OH) to the peak at *m/z* 608.2. Based upon the reasonable assumption that both unlabeled and labeled compounds were electrosprayed with similar ionization yields, relative concentration of each species were estimated to be such as 63.2% of CB[7]-(^{16}OH) and 36.8 % CB[7]-(^{18}OH). This shows that, beside the expected radical pathway (Scheme 3), nucleophilic addition of

water on a carbocation is expected to explain the presence of the observed non-labeled CB[7]-^{16}OH. This carbocation likely originates from the one-electron oxidation of CB[7]• radical. Thus, isotopic ^{18}O labeled experiments indicate that a significant part of the hydroxylation reaction takes place *via* an ionic mechanism (through CB[7]$^{+}$ cation) before probable nucleophilic addition of water. Finally, and even though several reaction parameters were investigated in detail, the high selectivity of the monohydroxylation reaction remains unclear. Further work is needed to fully address the observed results and possibly extend the scope of the reaction to directly introduce other functional groups.

CONCLUSION

In summary, the methods previously available for CB functionalization, although particularly elegant, relied either on a multiple-step sequence to introduce a functional monomer before macrocylic closing or on moderate yield reactions using S_2O_8 salts as radical initiator. However, we reported herein a method using a controlled generation of hydroxyl radicals from hydrogen peroxide, to rapidly obtaining each of the main members of the cucurbituril family as monohydroxy derivatives, including CB[8]-(OH), without contaminations by metal or alkaline salts. Calculations of bond dissociation energies (BDE) of the C-H_c, C-H_b and C-H_a carbon-hydrogen bonds revealed that the H_c position is the more prone to react and that, for CB[8], radicals generated from abstraction at position *b* are almost as stable as those generated from abstraction at position *c* likely opening a pathway for undesired reactions leading to decay products. As we anticipate an expanded use of monofunctional cucurbiturils as was seen for cyclodextrins a few decades ago, we believe that this method can be widely applied for the introduction of a variety of other functional groups on the exterior skeleton of cucurbiturils for targeted applications.

ASSOCIATED CONTENT

Supporting Information. The procedure for the preparation of CB[*n*]-(OH), ^{13}C NMR spectra, details of High Resolution MS analyses, decay products of CB[8], details for the calculations of BDEs and structures of each CB[*n*]• radical are given in the supporting information. CCDC numbers for the crystallographic files: 1052401 to 1052403. This material is available free of charge via the Internet at http://pubs.acs.org.

AUTHOR INFORMATION

Corresponding Authors

* Emails: david.bardelang@univ-amu.fr; olivier.ouari@univ-amu.fr.

Author Contributions

The manuscript was written through contributions of all authors. All authors have given approval to the final version of the manuscript.

ACKNOWLEDGMENT

We would like to thank Drs Christopher I. Ratcliffe and John A. Ripmeester for their help regarding an X-ray structure which greatly inspired this work. L.C. acknowledges support from Spectropole, the Analytical Facility of Aix-Marseille University, by allowing a special access to the instruments purchased with European Funding (FEDER OBJ2142-3341). We also aknowledge Pr. Didier Siri for his help regarding the calculations of bond dissociation energies and Dr. Stéphane Gastaldi for the use of the Rayonet reactor. CNRS, Aix-Marseille Université, and Région PACA (project "Masked Spins") are acknowledged for financial supports. The authors are also grateful to the EPR facilities available at the national TGE RPE at Aix-Marseille University.

REFERENCES

1. (a) Lagona, J.; Mukhopadhyay, P; Chakrabarti, S.; Isaacs, L. *Angew. Chem., Int. Ed.* **2005**, *44*, 4844−4870. (b) Lee, J. W.; Samal, S.; Selvapalam, N.; Kim, H.-J.; Kim, K. *Acc. Chem. Res.* **2003**, *36*, 621−630. (c) Kim, J.; Jung, I.-S.; Kim, S.-Y.; Lee, E.; Kang, J.-K.; Sakamoto, S.; Yamaguchi, K.; Kim, K. *J. Am. Chem. Soc.* **2000**, *122*, 540−541. (d) Ghale, G.; Nau, W. N. *Acc. Chem. Res.* **2014**, *47*, 2150–2159. (e) Yang, H.; Yuan, B.; Zhang, X.; Scherman, O. A. *Acc. Chem. Res.* **2014**, *47*, 2106–2115.
2. (a) Moghaddam, S.; Yang, C.; Rekharsky, M.; Ko, Y. H.; Kim, K.; Inoue, Y.; Gilson, M. K. *J. Am. Chem. Soc.* **2011**, *133*, 3570−3581. (b) Rekharsky, M. V.; Mori, T.; Yang, C.; Ko, Y. H.; Selvapalam, N.; Kim, H.; Sobransingh, D.; Kaifer, A. E.; Liu, S.; Isaacs, L.; Chen, W.; Moghaddam, S.; Gilson, M. K.; Kim, K.; Inoue, Y. *Proc. Natl. Acad. Sci. U. S. A.* **2007**, *104*, 20737−20742. (c) Hwang, I.; Baek, K.; Jung, M.; Kim, Y.; Park, K. M.; Lee, D.-W.; Selvapalam, N.; Kim, K. *J. Am. Chem. Soc.* **2007**, *129*, 4170−4171.
3. (a) Kim, H.-J.; Heo, J.; Jeon, W. S.; Lee, E.; Kim, J.; Sakamoto, S.; Yamaguchi, K.; Kim, K. *Angew. Chem., Int. Ed.* **2001**, *40*, 1526−1529. (b) Jeon, Y. J.; Bharadwaj, P. K.; Choi, S. W.; Lee, J. W.; Kim, K. *Angew. Chem., Int. Ed.* **2002**, *41*, 4474−4476.
4. (a) Lee, J. W.; Han, S. C.; Kim, J. H.; Ko, Y. H.; Kim, K. *Bull. Korean Chem. Soc.* **2007**, *28*, 1837−1840. (b) Wang, W.; Kaifer, A. E. *Angew. Chem., Int. Ed.* **2006**, *45*, 7042−7046.
5. (a) Reczek, J. J.; Kennedy, A. A.; Halbert, B. T.; Urbach, A. R. *J. Am. Chem. Soc.* **2009**, *131*, 2408−2415. (b) Heitmann, L. M.; Taylor, A. B.; Hart, P. J.; Urbach, A. R. *J. Am. Chem. Soc.* **2006**, *128*, 12574–12581.
6. (a) Zhang, J.; Coulston, R. J.; Jones, S. T.; Geng, J.; Scherman, O. A.; Abell, C. *Science* **2012**, *335*, 690−694. (b) Rauwald, U.; Scherman, O. A. *Angew. Chem., Int. Ed.* **2008**, *47*, 3950−3953.
7. Nguyen, H. D.; Dang, D. T.; van Dongen, J. L. J.; Brunsveld, L. *Angew. Chem., Int. Ed.* **2010**, *49*, 895−898.
8. Zhao, J.; Kim, H.-J.; Oh, J.; Kim, S.-Y.; Lee, J. W.; Sakamoto, S.; Yamaguchi, K.; Kim, K. *Angew. Chem., Int. Ed.* **2001**, *40*, 4233−4235.
9. (a) Isobe, H.; Sato, S.; Nakamura, E. *Org. Lett.* **2002**, *4*, 1287−1289. (b) Flinn, A.; Hough, G. C.; Stoddart. J. F.; Williams, D. J. *Angew. Chem., Int. Ed. Engl.* **1992**, *31*, 1475−1477.
10. (a) Mock, W. L.; Shih, N.-Y. *J. Org. Chem.* **1986**, *51*, 4440−4446. (b) Jiao, D.; Biedermann, F.; Tian, F.; Scherman, O. A. *J. Am. Chem. Soc.* **2010**, *132*, 15734−15743. (c) Kim, K. *Chem. Soc. Rev.* **2002**, *31*, 96−107.
11. (a) Kim, K.; Selvapalam, N.; Ko, Y. H.; Park, K. M.; Kim, D.; Kim, J. *Chem. Soc. Rev.* **2007**, *36*, 267−279. (b) Day, A. I.; Arnold, A. P.; Blanch, R. J. *Molecules* **2003**, *8*, 74−84.
12. (a) Lucas, D.; Minami, T.; Iannuzzi, G.; Cao, L.; Wittenberg, J. B.; Anzenbacher, P. Jr.; Isaacs, L. *J. Am. Chem. Soc.* **2011**, *133*, 17966−17976. This strategy has then been extended to prepare ammonium guests appended CB[6] and monofunctionalized CB[7] derivatives, see respectively (b) Cao, L.; Isaacs, L. *Org. Lett.* **2012**, *14*, 3072−3075. (c) Vinciguerra, B.; Cao, L.; Cannon, J. R.; Zavalij, P. Y.; Fenselau, C.; Isaacs, L. *J. Am. Chem. Soc.* **2012**, *134*, 13133−13140. (d) Cao, L.; Hettiarachchi, G.; Briken, V.; Isaacs, L.

Angew. Chem., Int. Ed. **2013**, *52*, 12033–12037.
13. Zhao, N.; Lloyd, G. O.; Scherman, O. A. *Chem. Commun.* **2012**, *48*, 3070−3072.
14. Jon, S. Y.; Selvapalam, N.; Oh, D. H.; Kang, J.-K.; Kim, S.-Y.; Jeon, Y. J.; Lee, J. W.; Kim, K. *J. Am. Chem. Soc.* **2003**, *125*, 10186−10187.
15. Ahn, Y.; Jang, Y.; Selvapalam, N.; Yun, G.; Kim, K. *Angew. Chem., Int. Ed.* **2013**, *52*, 3140−3144.
16. Ingold, K. U.; DiLabio, G. A. *Org. Lett.* **2006**, *8*, 5923−5925.
17. Zhu, X.; Fan, X.; Ju, G.; Cheng, M.; An, Q.; Nie, J.; Shi, F. *Chem. Commun.* **2013**, *49*, 8093−8095.
18. Fuenzalida, T.; Fuentealba, D.; *Photochem. Photobiol. Sci.* **2015**, *14*, 686-692.
19. (a) Bardelang, D.; Banaszak, K.; Karoui, H.; Rockenbauer, A.; Waite, M.; Udachin, K.; Ripmeester, J. A.; Ratcliffe, C. I.; Ouari, O.; Tordo, P. *J. Am. Chem. Soc.* **2009**, *131*, 5402−5404. (b) Bardelang, D.; Casano, G.; Poulhes, F.; Karoui, H.; Filippini, J.; Rockenbauer, A.; Rosas, R.; Monnier, V.; Siri, D.; Gaudel-Siri, A.; Ouari, O.; Tordo, P. *J. Am. Chem. Soc.* **2014**, *136*, 17570−17577. (c) Wang, R.; Bardelang, D.; Waite, M.; Udachin, K. A.; Leek, D. M.; Yu, K.; Ratcliffe, C. I.; Ripmeester, J. A. *Org. Biomol. Chem.* **2009**, *7*, 2435–2439. (d) Bardelang, D.; Udachin, K. A.; Anedda, R.; Moudrakovski, I.; Leek, D. M.; Ripmeester, J. A.; Ratcliffe, C. I. *Chem. Commun.* **2008**, 4927−4929.
20. (a) Hardy, M.; Bardelang, D.; Karoui, H.; Rockenbauer, A.; Finet, J.-P.; Jicsinszky, L.; Rosas, R.; Ouari, O.; Tordo, P. *Chem. − Eur. J.* **2009**, *15*, 11114−11118. (b) Hardy, M.; Chalier, F.; Ouari, O.; Finet, J.-P.; Rockenbauer, A.; Kalyanaraman, B.; Tordo, P. *Chem. Commun.* **2007**, 1083−1085. (c) Hardy, M.; Poulhés, F.; Rizzato, E.; Rockenbauer, A.; Banaszak, K.; Karoui, H.; Lopez, M.; Zielonka, J.; Vasquez-Vivar, J.; Sethumadhavan, S.; Kalyanaraman, B.; Tordo, P.; Ouari O. *Chem Res Toxicol.* **2014**, *27*, 1155-65.
21. Bardelang, D.; Finet, J.-P.; Jicsinszky, L.; Karoui, H.; Marque, S. R. A.; Rockenbauer, A.; Rosas, R.; Charles, L.; Monnier, V.; Tordo, P. *Chem.− Eur. J.* **2007**, *13*, 9344−9354.
22. Chalier, F.; Tordo, P. *J. Chem. Soc., Perkin Trans. 2* **2002**, 2110–2117.
23. Beckwith, A. L. J.; Bowry, V. W.; Ingold, K. U. *J. Am. Chem. Soc.* **1992**, *114*, 4983–4992.
24. (a) Isaacs, L. *Isr. J. Chem.* **2011**, *51*, 578–591. (b) Huang, W.-H.; Zavalij, P. Y.; Isaacs, L. *Polym. Prepr.* **2010**, *51*, 154–155. (c) Huang, W.-H.; Zavalij, P. Y.; Isaacs, L. *Angew. Chem., Int. Ed.* **2007**, *46*, 7425–7427. (d) Huang, W.-H.; Liu, S.; Zavalij, P. Y.; Isaacs, L. *J. Am. Chem. Soc.* **2006**, *128*, 14744–14745.
25. Wu, A.; Chakraborty, A.; Witt, D.; Lagona, J.; Damkaci, F.; Ofori, M. A.; Chiles, J. K.; Fettinger, J. C.; Isaacs, L. *J. Org. Chem.* **2002**, *67*, 5817–5830.

Graphical Abstract